Analysis of the Stepped-Impedance Low Pass Filter using Sub-Gridding Finite-Difference Time-Domain Method

서브 그리딩 유한 차분 시간 영역법을 이용한 계단형 임피던스 저역 통과 필터 해석

Berm-Seok Noh · Jae-Hoon Choi · Sang-Sun Lee · Je-myung Jeong

노범석 · 최재훈 · 이상선 · 정제명

Abstract

One of the dominant aspects governing the accuracy of the FDTD method is the size of the spatial increment used in the model. The effect of having reduced cell size is to increase the computational time and memory requirements. To overcome these problems, sub-gridding technique can be used. This implies that the application of a sub-grid cell would provide improved accuracy without increasing the run time and computer resources considerably. In this paper, we describe the three dimensional sub-gridding technique that is applied to model only the fine structure region of interest. The detailed solution procedure is described and some test geometries were solved by both uniform grid and sub-grid models to validate the suggested approach. While keeping the accuracy, the computational time becomes 6 times faster and the memory requirement is reduced by a factor of 2.5 comparing to the conventional FDTD approach.

Key words : sub-gridding, subcell.

요 약

FDTD 해석법에서 공간적 셀의 크기는 해석의 정확도를 결정하는 중요한 요소이다. 하지만 정확도를 향상시키기 위하여 셀의 크기를 줄이게 되면, 해석시간과 기억용량의 증가를 초래하게 되는데 서브 그리딩을 사용하여 이를 해결할 수 있다. 본 논문에서는 관심영역만 세밀하게 해석할 수 있는 3차원 서브 그리딩법을 기술하고 이를 응용하여 몇 가지의 구조를 해석하였다. 제안한 방법의 타당성을 확인하기 위하여 균일 그리딩과 서브 그리딩을 적용하여 특성을 해석하고 그 결과를 비교하였다. 제안한 방법을 사용하였을 경우 동일한 정확도에서 균일 그리딩에 비하여 6배의 해석시간의 줄었고 기억용량은 2.5배 정도 줄어들었다.

Ⅰ. Introduction

The FDTD method has been successfully used to analyze the properties of various microwave structures. One of dominant aspect governing the accuracy of the FDTD is the size of the spatial increment used in the model. In some structures, FDTD cell size may be determined by geometry features rather than by cell size requirement. For example, for a stepped impedance filter, the strip width is smaller than the minimum cell size of conventional FDTD. By reducing the cell size to obtain the accurate result

「This work was supported by Hanyang University, Korea, made in the program year of 2000.」

한양대학교 전자전기컴퓨터공학부(Department Radio Science and Engineering, Hanyang University)

· 논 문 번 호 : 20011031-152

· 수정완료일자 : 2002년 1월 30일

of this type of problem, the run time and memory requirement increase substantially. Therefore, one needs to use a sub-gridding algorithm to improve the accuracy and to reduce computational time and memory size simultaneously. A few paper have been published on sub-gridding FDTD algorithm [1]~[4]. In [1]~[3], electric field on the sub-grid boundary were calculated using the homogeneous traveling wave equation. The homogeneous traveling wave equation must assume a homogeneous medium. In [4], magnetic fields set on sub-grid boundary to satisfy normal field continuity between the two media.

Since the error occurred by not satisfying the boundary condition is not significant, we suggest a sub-gridding algorithm placing electric fields on sub -grid boundary unlike [4] in this paper. To reduce error by not satisfying the boundary condition, weighting factor is utilized. By doing this, one can remove the limitation imposed in [1]~[3]. To verify the validity of this algorithm, a waveguide and stepped impedance filter characteristics are analyzed.

Ⅱ. Algorithm of the Sub-Gridding Technique

This algorithm is based on the finite-difference representation of Maxwell's equations using a central -difference formation and the Yee-cell notation [5]. In the sub-gridding algorithm, it is necessary to match coarse cell and fine cell at sub-grid boundary. Also, the cell size in the fine grid region should be an odd integer fraction of the coarse cell size, 1/3, 1/5, 1/7 and so on. Hence, it provides collocated fields in time and space between coarse grid and fine grid. In this paper, as shown Fig. 1, fine cell size is 1/3 of the coarse cell size. The time increment in the fine cell region, Δt_f is one-third of the coarse grid time increment, Δt.

To calculate the sub-grid fields, values of the fields at and near the sub-grid boundary are needed. We define the electric fine grid field as "e", the magnetic fine grid field as "h", the electric coarse grid field as "E", and the magnetic coarse grid field as "H".

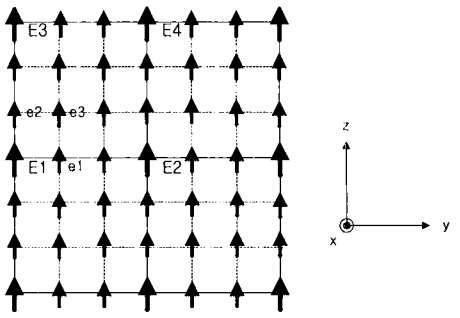

Fig. 1. A section of the sub-grid boundary (front view).

2-1 Sub-gridding Algorithm

The algorithm illustrated in Fig. 2 can be summarized as following.

(1) Calculate $H^{n+1/2}$ and E^{n+1}.
(2) Calculate $h^{n+1/6}$ using e^n calculated by n time step.
(3) Calculate $e^{n+2/6}$ using $h^{n+1/6}$ calculated by step (2). $e^{n+2/6}$ fields located on the sub-grid region boundary are calculated by spatial and time interpolation of E^{n-1}, E^n, and E^{n-1}.

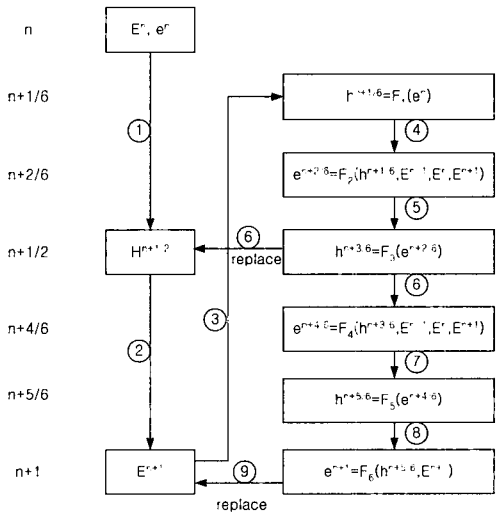

Fig. 2. Sub-gridding algorithm flow chart.

(4) Calculate $h^{n+3/6}$ using $e^{n+2/6}$ calculated by step (3). Replace $H^{n+1/2}$ by collocated $h^{n+3/6}$ in sub-grid regions.

(5) Calculate $e^{n+4/6}$ using $h^{n+3/6}$ calculated by step (4). $e^{n+4/6}$ fields located on the sub-grid region boundary are calculated by spatial and time interpolation of E^{n-1}, E^n, and E^{n+1}.

(6) Calculate $h^{n+5/6}$ using $e^{n+4/6}$ calculated by step (5).

(7) Calculate e^{n+1} using $h^{n+5/6}$ calculated by step (6). e^{n+1} fields located on the sub-grid region boundary are calculated by spatial interpolation of E^{n+1}.

Replace E^{n+1} by collocated e^{n+1} in sub-grid regions.

Repeat procedure from step (1) to step (7).

2-2 Fields Interpolation

In steps, (3), (5), (7), the value of e fields including e fields at sub-grid boundary have to be calculated but boundary e fields can not be calculated by FDTD equation because h fields outside sub-grid region do not exist. Therefore in these time steps, e fields on the boundary are found by spatial interpolation technique using E fields on the boundary. For example, e^n on the boundary is calculated by nearest E^n on the boundary. But because $E^{n+2/6}$ is not calculated, $e^{n+2/6}$ can't be calculated. The same is true for $e^{n+4/6}$ fields.

2-2-1 Time Interpolation

To calculate $E^{n+2/6}$ and $E^{n+4/6}$ on the sub-grid boundary in these times, a second-order Taylor series expansion is used. Using the second-order Taylor series gives, E^{n+v} is given by

$$E^{n+v} = E^n + Av + \frac{Bv^2}{2} \tag{1}$$

where,

$$A = -\frac{E^{n+1}}{2} - \frac{E^{n-1}}{2} \tag{2}$$

$$B = E^{n+1} + E^{n-1} - 2E^n \tag{3}$$

$v = 2/6, 4/6.$

2-2-2 Spatial Interpolation

Non-collocated e fields on the sub-grid boundary are calculated using spatial interpolation of E. The interpolated fields are only tangential fields to the sub-grid boundary. A straightforward spatial interpolation is used. All other sub-grid region fields out of sub-grid boundary are calculated by FDTD equations.

The non-collocated sub-grid boundary fields are calculated by a straightforward spatial interpolation of the four surrounding E fields. Fig. 1 shows a section of the sub-grid boundary surface. Referring to Fig. 1, interpolation equations to calculate non-collocated e are given by

$$\begin{aligned} e_1^{n+v} &= \frac{2}{3}E_1^{n+v} + \frac{1}{3}E_2^{n+v} \\ e_2^{n+v} &= \frac{2}{3}E_1^{n+v} + \frac{1}{3}E_3^{n+v} \\ e_3^{n+v} &= \frac{1}{3}E_1^{n+v} + \frac{2}{3}\frac{E_1^{n+v} + E_2^{n+v} + E_3^{n+v} + E_4^{n+v}}{4} \end{aligned} \tag{4}$$

The interpolated fields given by the above equations are examples and must also be applied to calculate other fields and then h fields can be

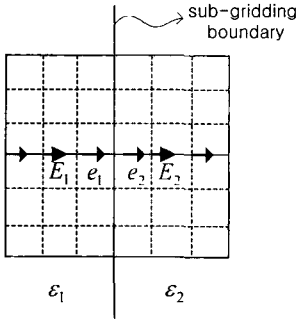

Fig. 3. Two different material regions normal to the sub-gridding boundary.

calculated. But when the sub-gridding boundary is placed normal to the two different media as illustrated in Fig. 3, normal component of electric field is not satisfy the continuity condition. However due to this problem is not significant, weighting factor is used in order to enhance stability.

2-2-3 Stability Enhancement

In order to increase the stability of the proposed sub-grid algorithm, the weighting schemes are suggested based on the experiment.

2-2-3-1 e weighting

The differences between the method that calculates the sub-grid boundary fields and the method that calculates the rest of e fields in the fine grid generate some instability. To increase stability, the following approach is adopted. Fig. 4 shows schematic of the electric fields propagating in x-direction in the sub-grid region. The fine grid electric fields of the first cell inside the overlapping region are weighted as following.

$$
\begin{aligned}
e_1^{n+v} &= \alpha e_1^{n+v} + \beta \frac{E_1^{n+v} + e_2^{n+v}}{2} \\
e_4^{n+v} &= \alpha e_4^{n+v} + \beta \frac{e_3^{n+v} + e_5^{n+v}}{2} \\
&\bullet \\
&\bullet \\
&\bullet
\end{aligned}
\qquad (5)
$$

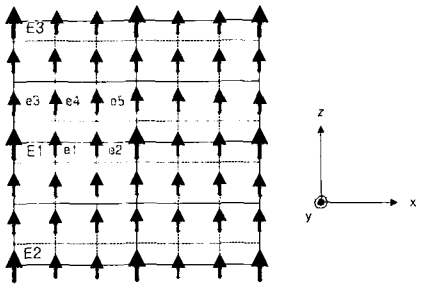

Fig. 4. Schematic illustration of the electric fields in the x-z plane of the sub-grid region (side view).

The procedure given by equation (5) is performed at every fine grid time step.

Fig. 5 illustrates the stability enhancement with varying weighting factors. When weighting factors are not applied, stable time is less than 4000 time steps. However when weighting factors are applied, stable time is increased.

As shown Fig. 5, stability is guaranteed for and . In this case, stable time is about 10000 time steps.

2-2-3-2 H weighting

In Fig. 6, magnetic fields in the x-z plane within the sub-grid region are illustrated. The coarse grid magnetic fields of the first coarse cell inside the overlapping region are weighted as following.

$$
\begin{aligned}
H_2^{n+1/2} &= 0.01 H_{2,coarse}^{n+1/2} + 0.99 h_{2,fine}^{n+1/2} \\
h_2^{n+1/2} &= 0.01 H_{2,coarse}^{n+1/2} + 0.99 h_{2,fine}^{n+1/2} \\
H_4^{n+1/2} &= 0.01 H_{4,coarse}^{n+1/2} + 0.99 h_{4,fine}^{n+1/2} \\
h_4^{n+1/2} &= 0.01 H_{4,coarse}^{n+1/2} + 0.99 h_{4,fine}^{n+1/2} \\
&\bullet \\
&\bullet \\
&\bullet
\end{aligned}
\qquad (6)
$$

where, $H_{2coarse}$, h_{2fine}, $H_{4coarse}$, and h_{4fine} are calculated values by the Yee FDTD equations at n+1/2 time step.

Ⅲ. Waveguide Analysis

The waveguide structure operating at 9.26 GHz excited by TE_{10} mode sinusoidal source was modeled as shown in Fig. 7. The structure is modeled by 42 $\Delta x \times 22 \Delta y \times 50 \Delta z$. The fine grid region is modeled by $9 \Delta x \times 5 \Delta y \times 10 \Delta z$ located at the central part of the waveguide. Uniform grid model was created with a cell size of 2.16 mm and sub-grid model was created with a fine cell size of 0.72 mm and a coarse sell size of 2.16 mm.

For comparison, magnitude of the electric field in the fine grid region was compared to the correspond-

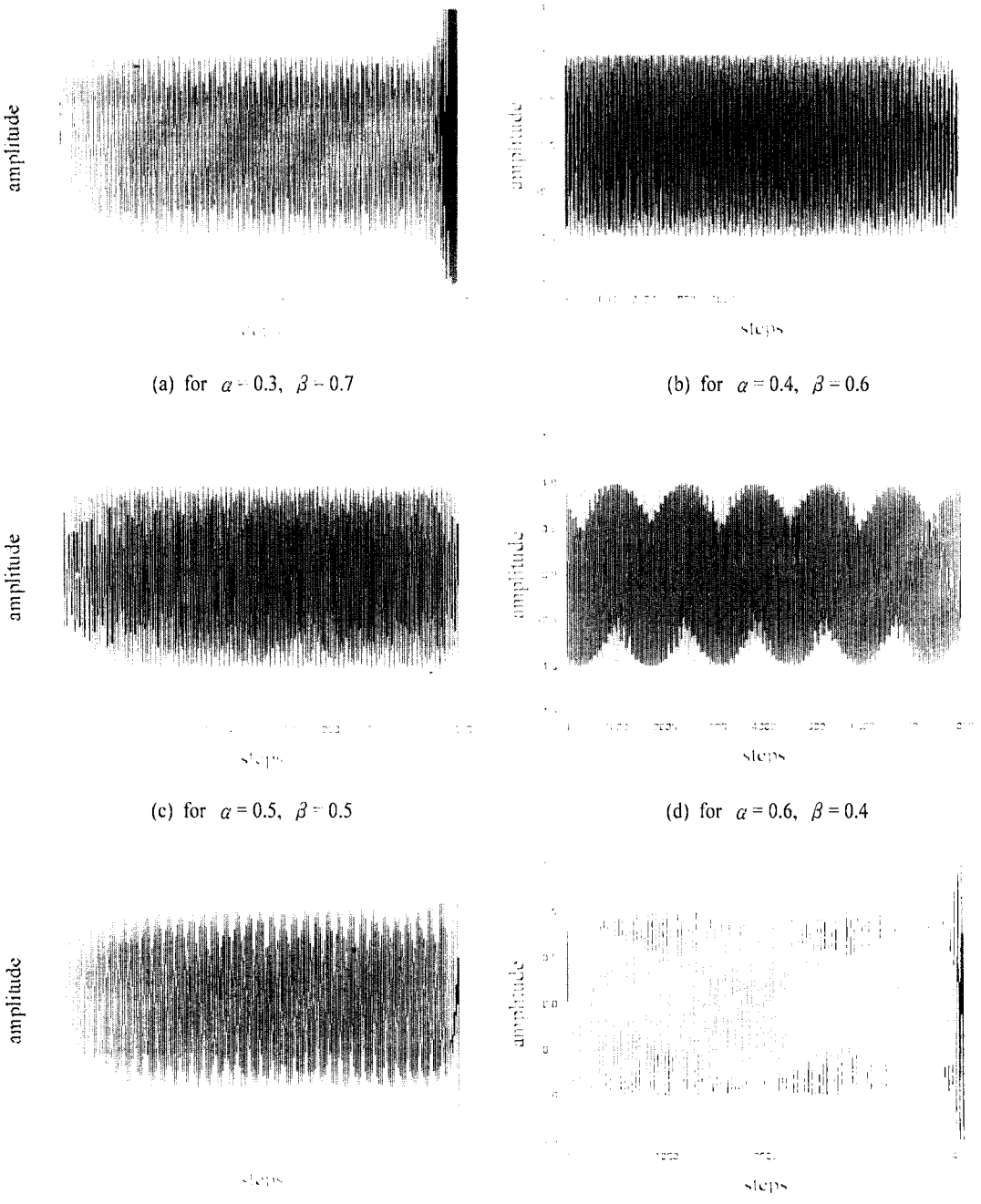

(a) for $\alpha = 0.3$, $\beta = 0.7$

(b) for $\alpha = 0.4$, $\beta = 0.6$

(c) for $\alpha = 0.5$, $\beta = 0.5$

(d) for $\alpha = 0.6$, $\beta = 0.4$

(e) for $\alpha = 0.7$, $\beta = 0.3$

(f) for $\alpha = 1$, $\beta = 0$

Fig. 5. stability enhancement with varying weighting factors.

ing values determined by the uniform grid algorithm in Fig. 8.

Amplitude error between the two approaches is computed by

$$error_{mag} = \left| \frac{E_{uniform} - E_{subgrid}}{E_{uniform}} \right| \times 100\% \quad (7)$$

The maximum error between the two model is

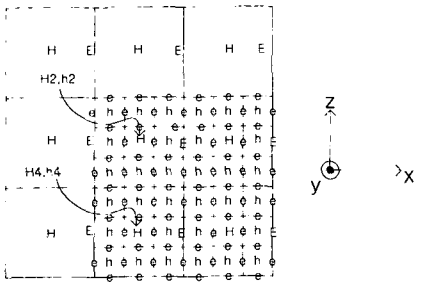

Fig. 6. Schematic illustration of the magnetic fields in the x-z plane of the sub-grid region (side view).

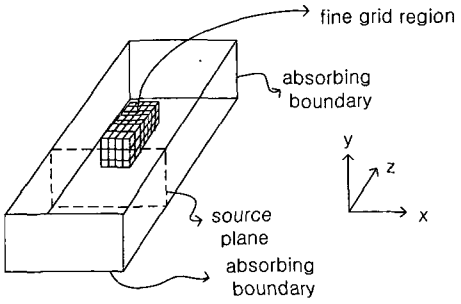

Fig. 7. Schematic illustration of the waveguide.

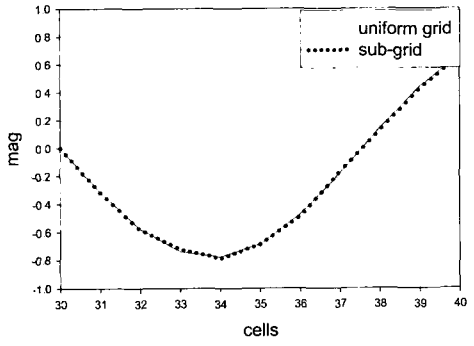

Fig. 8. "+z" directed wave propagation in sub-grid region for two case.

about 0.5 %.

Ⅳ. Analysis of the Stepped-Impedance Low Pass Filter using Subgridding Algorithm

We analyzed a low-pass filter having a maximally flat in-band response and a cutoff frequency of 2.5 GHz[6] by the proposed method. It is required that the insertion loss at 4 GHz is more than 20 dB. The filter impedance is 50Ω; the highest practical line impedance is 150Ω, and the lowest is 10Ω. Relative permittivity of the substrate is 3.5. Fig. 9 is the schematic illustration of the filter modeled by the sub-gridding algorithm. The impedance value of 1, 3, 5 steps is 10 Ω and the impedance value of 2, 4, 6 steps is 150 Ω. Therefore, the thickness of 2, 4, 6 steps is thinner than the thickness of 1, 3, 5 steps. To model such a planar structure, it requires a large number of cells. However, it is possible to model this structure using sub-gridding technique. Calculations were made for three cases, i.e., full coarse grid, sub-grid, and full fine grid. The coarse grid were modeled with 0.26 mm cell size for x, 0.64mm cell size for y, 0.254 mm cell size for z and the fine grid used $\Delta x/3$ for x, $\Delta y/3$ for y, $\Delta z/3$ for z. Dimension of full coarse grid and full fine grid were $48\Delta x \times 75\Delta y \times 15\Delta z$ and $98\Delta x \times 155\Delta y \times 20\Delta z$, respectively. For sub-grid, the fine grid fills space of $4\Delta x \times 39\Delta y \times 3\Delta z$ coarse grid cells.

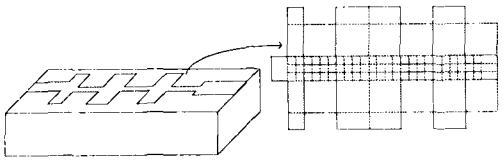

Fig. 9. Schematic illustration of the stepped-impedance low pass filter.

S_{21} values obtained using the FDTD with a coarse grid, fine grid, and sub-grid calculation are shown in Fig. 10. S_{21} becomes greater than 0 dB at around 1 GHz. This error is due to the reflection at the sub-grid boundary caused by using the weighting factor. However the error is not significant. The use of the sub-grid reduces required memory and run time while it provides accuracy comparable to a single uniform grid with the fine cell. The run times for the three test cases are listed in Table 1. As shown in Table 1, it takes about 20 hours for fine grid, about

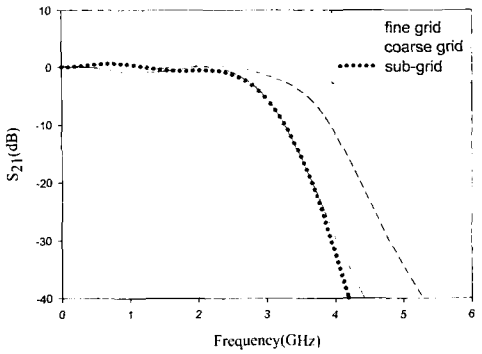

Fig. 10. S_{21} of the stepped-impedance low-pass filter.

Table 1. Run times for the three test cases.

Test case	Run time
Coarse grid	1h 43 m
Sub-grid	3h 47 m
Fine-grid	20 h

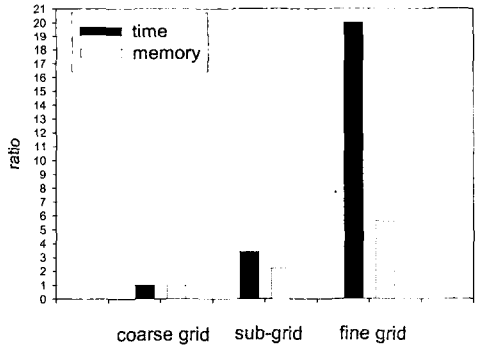

Fig. 11. Normalized run times and memory requirements for three test cases.

3 hours 47 minutes for sub-grid, and about 1 hour 43 seconds for coarse grid for the same accuracy.

The normalized run times and required memory sizes for three models are compared in Fig. 11. Both the required memory and the run time for the sub-grid test case were greatly below those of the fine grid.

V. Conclusion

An algorithm for incorporating sub-gridding technique into finite-difference time-domain method has been suggested. A procedure to update the field values within coarse grid region was implemented. Stability considerations were also discussed. For a waveguide structure, the amplitude error was about 0.5 % and for filter structure, the run time and memory size are reduced substantially while keeping the accuracy almost the same as that of fine grid algorithm. Therefore, accurate analysis is possible without modeling the whole space with the fine grid cell.

VI. References

[1] S. S. Zivanovic, K. S. Yee, and K. K. Mei, "A subgridding method for the time-domain finite-difference method to solve Maxwell's equations", *IEEE Trans. Microwave Theory Tech.*, vol. 39, pp. 471-479, Mar. 1991.

[2] D. T. Prescott and N. V. Shuley, "A method for incorporating different sized cells into the finite-difference time-domain analysis technique", *IEEE Microwave Guided Wave Lett.*, vol. 2, pp.434-436, Nov. 1992.

[3] Mikel J White, Magdy F. Iskander and Zhenlong Huang, "Development of a Multigrid FDTD Code for Three-Dimensional Application", *IEEE Transactions On Antennas And Propagation*, vol. 45, no. 10, pp. 1512-1517, Oct. 1997.

[4] Michae W. Chevailer, Raymond J. Luebbers, "FDTD Local Grid with Material Traverse", *IEEE Transactions On Antennas And Propagation*, vol. 45, pp. 411-421, Mar. 1997.

[5] Allen Taflove, *Computational Electrodynamics: the finite-difference time-domain method*, Artech House, 1995.

[6] David M. Pozar, "*Microwave engineering*", Wiley, pp. 470-473, 1998.

노 범 석

2000년: 경희대학교 전자공학과 (공학사)
2002년: 한양대학교 전자통신전파 공학과 (공학석사)
2002년 ~ 현재: LG전자
[주 관심분야] 전자파 수치해석

이 상 선

1978년: 한양대학교 전자공학 (공학사)
1983년: 한양대학교 전자공학 (공학석사)
1990년: University of Florida 전기공학 (공학박사)
1991년 4월 ~ 1991년 11월: 생산기술연구원 선임연구원겸 조교수
1991년 11월 ~ 1993년 2월: 전자부품종합기술 연구소 선임연구원
1993년 3월 ~ 현재: 한양대학교 전자전기공학부 부교수.
[주 관심분야] 광전집적회로, 광통신소자 및 마이크로파 시스템

최 재 훈

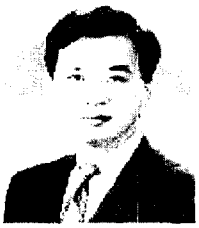

1980년: 한양대학교 전자공학과 (공학사)
1986년: 미국 Ohio University 전기공학과 (공학석사)
1989년: 미국 Ohio University 전기공학과 (공학박사)
1989년 ~ 1991년: 미국 Arizona State University 연구교수
1991년 ~ 1995년: 한국통신 위성사업본부 연구팀장
1995년 ~ 현재: 한양대학교 전자전기컴퓨터공학부 부교수
[주 관심분야] 안테나 설계 및 분석, 마이크로파 능·수동 소자 설계, 전파전파 모델링

정 제 명

현재: 한양대학교 전자전기컴퓨터공학부 부교수
[주 관심분야] 광소자 및 마이크로파 시스템